Structural and Morphological Transformations in Self-assembled Sn Quantum Dots in Si matrix

P. Möck[1], Y. Lei[2], T. Topuria[2], N.D. Browning[2], R. Ragan[3*], K.S. Min[3**], and H.A. Atwater[3]

[1] Portland State University, Department of Physics, P.O. Box 751, Portland, OR 97207-0751, pmoeck@pdx.edu
[2] Department of Physics, University of Illinois at Chicago, 845 W. Taylor Street, Chicago, Illinois 60607-7059
[3] Thomas J. Watson Laboratory of Applied Physics, California Institute of Technology, MS 128-95, Pasadena, CA 91125
* now at: Hewlett-Packard Laboratories M/S 1123, 1501 Page Mill Rd, Palo Alto, CA 94304, ** now at: Intel Corporation, California Technology and Manufacturing, MS RNB-2-35, 2200 Mission College Blvd, Santa Clara, CA 95052-8119

ABSTRACT

The thermodynamics of misfitting precipitates provide reasonable explanations for structural and morphological transformations of Sn (rich) quantum dots in Si matrix that were observed by means of atomic resolution Z-contrast scanning transmission electron microcopy. Morphological transformations (within the diamond structure) from tetrakaidecahedrons to octahedrons with the precipitate size are explained by an increasing contribution of the elastic mismatch energy to the Gibbs free energy. A simple estimate shows that an excess Gibbs free energy of approximately 0.4 eV per atom, corresponding to a hydrostatic pressure of about 19 GPa, can be released by a structural transformation from a quantum dot with diamond structure to a precipitate with β-Sn structure and a lattice mismatch strain minimizing orientation relationship with the surrounding Si matrix.

Keywords: Sn quantum dots, endotaxy, Si

1. INTRODUCTION

Since bulk α-Sn (grey tin) is a direct, 0.08 eV, band gap semiconductor and bulk substitutional Sn_cSi_{1-c} solution are predicted to possess direct band gaps for $0.9 < c < 1$ [1], endotaxially grown quantum dots (QDs) in Si matrix consisting of pure α-Sn or substitutional Sn_ySi_{1-y} solutions with a sufficiently high Sn content may find applications in optoelectronic and thermo-photovoltaic devices that could be mass produced by means of the mature Si integrated circuit technology. There is, however, a 41.8 % bulk unit cell volume mismatch between α-Sn and Si and the bulk equilibrium solid solubility of Sn in Si is only 0.12 % at room temperature. These limitations restrict growth of pseudomorph Sn_xSi_{1-x} layers on Si by molecular beam epitaxy (MBE) to a Sn content of about 10 % and a thickness of the order of magnitude 10 nm.

At MBE growth temperatures in the range 220 to 295 °C, pseudomorph Sn_xSi_{1-x} layers with up to 5 % Sn content have been grown to film thicknesses of up to 170 nm. Thermal treatments of these layers at temperatures above 500 °C for 1 hour lead to the formation of α-Sn precipitates, β-Sn precipitates, precipitates that consisted of both α-Sn and β-Sn, and misfit dislocations [2-4]. While these α-Sn precipitates could be considered to constitute QDs in this material system, the simultaneously present misfit dislocations are clearly undesirable for device applications.

Alternatively, temperature and growth rate modulated MBE [5,6] produces Sn_xSi_{1-x}/Si quantum well structures with essentially pseudomorph Sn_xSi_{1-x} substitutional solutions that possess Sn contents in the range of $x = 0.02$ to 0.05 and film thicknesses ranging from 1 to 2 nm. The growth temperatures of the Sn_xSi_{1-x} layers ranged from 140 to 170 °C and the growth rate was 0.02 nm s^{-1}. The Sn_xSi_{1-x} layers were overgrown with 4 to 6 nm of Si at the Sn_xSi_{1-x} growth temperature and at growth rates ranging from 0.01 to 0.03 nm s^{-1}. The temperature was then raised to 550 °C and a Si spacer/capping layer with a thickness of the order of magnitude 100 nm was grown at a rate of 0.05 nm s^{-1}. By the time this growth sequence had been completed, the Sn_xSi_{1-x} layer had experienced an *in situ* thermal treatment at 550 °C for a time of the order of magnitude 30 minutes. For the growth of Sn_xSi_{1-x}/Si multi-quantum well structures, the whole growth sequence was repeated several times, effectively resulting in an *in situ* thermal treatment for the first Sn_xSi_{1-x} layer at 550 °C for a time on the order of magnitude a few hours [5,6]. In addition to this *in situ* thermal treatment, *ex situ* anneals at temperatures between 550 and 900 °C were performed for 30 minutes.

Two different kinds of Sn precipitation (QD formation) mechanisms have recently been observed by means of analytical transmission electron microcopy (TEM) to operate simultaneously in this material system [7-9]. While α-Sn QDs grow by a void mediated formation mechanism in the Si spacer layers, QDs that consist of substitutional Sn_ySi_{1-y} ($y > x$) solutions grow from predecessor Sn_xSi_{1-x} layers by means of phase separation.

We observed recently in Sn_xSi_{1-x}/Si multi-quantum well structures a few years after the growth β-Sn (white tin) structure precipitates, precipitates with unidentified structure, and diffraction patterns that are consistent with ordered Sn-Si compounds [7], suggesting that there are probably structural transformations in this material system over sufficiently long times even at room temperature. Our recent observations also suggest that there are morphological transformations within the diamond structural prototype with increasing size of the QDs [8].

The present paper will briefly illustrate the state of the art in the field of endotaxially grown Sn (rich) QDs in Si and attempts to give explanations on the basis of the thermodynamics of misfitting precipitates for the above

mentioned recent observations of morphological and structural transformations.

2. EXPERIMENTAL DETAILS

Three (001) multi-quantum well structures with four embedded Sn_xSi_{1-x} layers and substitutional Sn contents of 2 %, 5 %, and 10 % in each of the Sn_xSi_{1-x} layers were grown at the California Institute of Technology by temperature and growth rate modulated MBE, subjected to an additional *ex-situ* anneal for 30 minutes at 800 ºC [5,6], stored at room temperature for a few years, and eventually selected for our analytical TEM investigations.

Our structural and (electron energy loss) spectroscopic analyses at the University of Illinois at Chicago employed both a JEOL JEM-2010F Schottky field emission STEM/TEM and a JEOL JEM-3010 TEM [7-9]. Parallel illumination TEM utilized conventional diffraction contrast imaging, selected area electron diffraction, and high-resolution phase contrast imaging. Atomic resolution Z-contrast imaging (also known as high angle annular dark field imaging) in the scanning probe mode (STEM) proved to be especially useful for our investigations as the effects of strain fields in and around QDs and interference effects such as the formation of moiré fringe due to double diffraction are negligible. TEM/STEM specimen preparation followed standard procedures involving mechanical grinding and ion milling.

3. RESULTS AND DISCUSSIONS

Fig. 1a shows a $Sn_{0.1}Si_{0.9}$/Si multi-quantum well structure in a Z-contrast STEM overview. Due to the nature of this contrast, the remains of the $Sn_{0.1}Si_{0.9}$ layers appear in this image brighter than the surrounding Si matrix since the average atomic number in these layers is much larger than that of Si. Most of the QDs formed at or in close proximity to the $Sn_{0.1}Si_{0.9}$ layer, but there are also many QDs that grew within the Si spacer layers. While Fig. 1b goes to show the void mediated formation mechanism by with α-Sn QDs grow in the Si spacer layers [9], Fig. 2a indicates the formation of substitutional Sn_ySi_{1-y} ($y > x$) solution QDs by means of phase separation [7,8].

It is now important to realize that the equilibrium shape of a void in Si has been determined experimentally [10] to be a tetrakaidecahedron, Fig. 2b. This shape is determined by {111}, i.e. octahedron, and {100}, i.e. cube, planes. $A = {}^{t}/_{a}$ is a shape parameter; for $A = 0$ the shape is an octahedron and $A = {}^{2}/_{3}$ corresponds to a cube.

The applications of Neumann's symmetry principle [11]:

$$\frac{4}{m}\bar{3}\frac{2}{m} \cap \frac{4}{m}\bar{3}\frac{2}{m} = \frac{4}{m}\bar{3}\frac{2}{m},$$

(where the operator $\cap$ stands for intersection) to the determination of the shape of α-Sn and Sn_ySi_{1-y} precipitates in a Si matrix shows that this is also a tetrakaidecahedron. Since the stress (pressure) is essentially hydrostatic, i.e. isotropic, Curie's symmetry principle [11]:

$$\infty\infty\infty\infty \cap \frac{4}{m}\bar{3}\frac{2}{m} = \frac{4}{m}\bar{3}\frac{2}{m}$$

yields no influence of the misfit stress field on the anisotropy of the interface energy density.

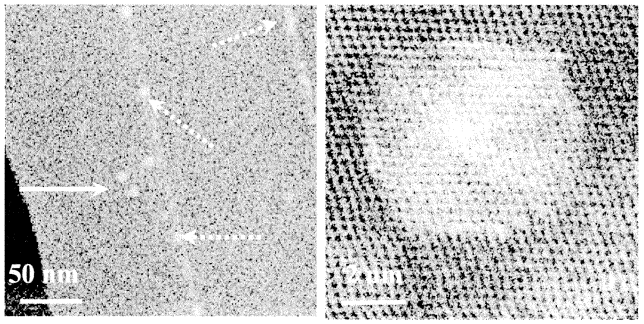

Figure 1: [110] cross section Z-contrast STEM images of $Sn_{0.1}Si_{0.9}$/Si multi-quantum well structures; **(a) right,** overview, while the full line arrow points towards a group of two QDs that grew within the Si spacer layer by means of the void mediated formation mechanism, the three broken line arrows point towards QDs that grew by phase separation at the level of the original $Sn_{0.1}Si_{0.9}$ layers; **(b) left,** void that is at its interface with the Si matrix lined by Sn, showing evidence for the operation of the mechanism by with α-Sn QDs grow.

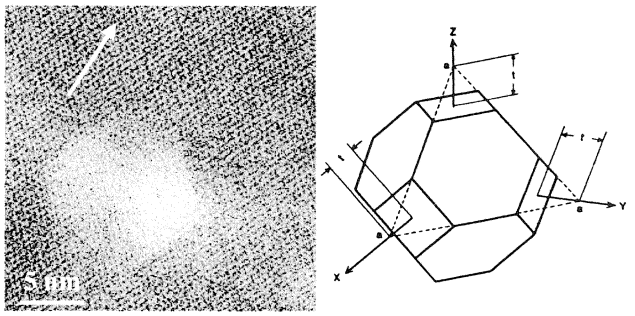

Figure 2: (a) right, [110] cross section Z-contrast STEM image of a substitutional Sn_ySi_{1-y} solution QD (with a high Sn content, $y > x = 0.1$) at the level of the former Sn_xSi_{1-x} layer, demonstrating the operation of the phase separation mechanism by which such QDs grow. The arrow represent the direction of the epitaxial deposit growth normal, (001), perpendicular to the remains of the Sn_xSi_{1-x} layer; **(b) left,** sketch of a tetrakaidecahedron with shape parameter annotation, reproduced (with permission) from ref. [11].

While the thermodynamics of smaller misfitting precipitates are likely to be determined by the contribution of the interface energy (which is proportional to the precipitate's interface area) to the Gibbs free energy, the thermodynamics of larger misfitting precipitates in the same two phase system are likely to be determined by the contribution of the elastic mismatch energy (which is proportional to the precipitate's volume) to the Gibbs free energy. Because of this, the shapes of smaller misfitting precipitates are likely to be dominated by the anisotropy of

the interface energy, while the shapes of larger misfitting precipitates in the same two phase systems are likely to be dominated by the anisotropy of the elastic mismatch energy [11].

A shape transition with size of Sn (rich) precipitates that is probably due to an increasing contribution of the elastic mismatch energy to the Gibbs free energy of the QDs has indeed been observed [8]. While smaller precipitates, Fig. 3a, possess the typical tetrakaidecahedron shape, (which probably results from the anisotropy of the interface energy density), a much larger precipitate, Fig. 3b, had a shape that resembles more closely an octahedron. The shape of this large precipitate probably results from the anisotropy of the elastic mismatch energy.

Intermediately sized Sn (rich) precipitates possessed tetrakaidecahedron shapes with smaller {001} facets, i.e. smaller shape parameters A, indicating a gradual transition to the shape of an octahedron (A = 0) with increasing size. As the large precipitate in Fig. 3b was partly observed at the predecessor substitutional $Sn_{0.1}Si_{0.9}$ solution layer and partly within the Si spacer layer, it may have grown by the simultaneous operation of both of the formation mechanisms, mentioned above. The upper part of the QD may, therefore, consist of α-Sn and the lower part of a substitutional Sn_ySi_{1-y} solution with a high Sn content. This hypothesis is consistent with the contrast in the image shown in Fig. 3b.

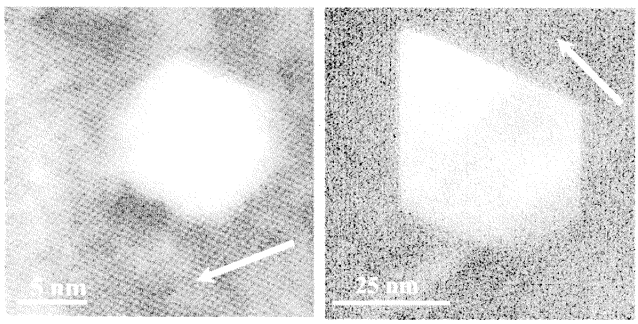

Figure 3: [110] cross section Z-contrast STEM images demonstrating the shape transition of the misfitting Sn (rich) precipitates with size; **(a) right,** from a tetrakaidecahedron as dominated by the anisotropy of the interface energy density to; **(b) left,** essentially an octahedron, as dominated by the anisotropy of the elastic mismatch energy. The arrows represent the respective directions of the epitaxial deposit growth normals, (001), perpendicular to the remains of the $Sn_{0.1}Si_{0.9}$ layers.

Structural transformations, Figs. 4a and b, in this material system are probably also driven by thermodynamics as there is a rather large contribution of the lattice mismatch energy to the Gibbs free energy. This contribution to the Gibbs free energy is simply the product of the pressure on the QD times its volume. Assuming that the pressure is hydrostatic one can replace this product by the product of the bulk modulus (B) and the volume change (ΔV). The usage of this simple formula for QDs is justified by studies of the size dependency of elastic properties of nanometer sized particles [12].

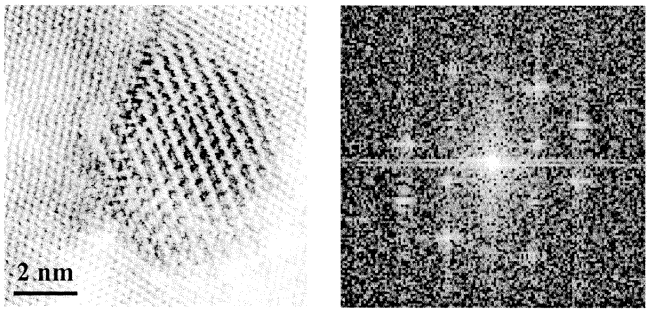

Figure 4: β-Sn structure precipitate in Si matrix, [110] cross section; **(a) right,** bright field STEM image **(b) left,** power spectrum (of the corresponding high angle annular dark field image). The strain minimizing orientation relationship is: $(011)_{\beta\text{-Sn}} \| (002)_{Si}$, $(600)_{\beta\text{-Sn}} \| (\bar{4}40)_{Si}$, and $[0\bar{7}7]_{\beta\text{-Sn}} \| [660]_{Si}$, where the symbol ‖ stands for parallel [13]. The shape of the precipitate is a rhombic dipyramidal polyhedron, in agreement to the application of Neumann's symmetry principle for the case of negligible elastic mismatch energy influences [14].

Approximating an α-Sn QD in this material system to a sphere of 10 nm diameter, which consists of about 21739 atoms, one obtains for an α-Sn QD (bulk modulus 42.6 GPa), with is strained to possess a lattice constant of 0.57516 nm [15], an elastic mismatch energy of 0.44 eV per atom. This excess Gibbs free energy corresponds to a compressive hydrostatic pressure of 18.6 GPa on the QD. For a Sn rich QD, the elastic mismatch energy and the corresponding pressure are estimated to be of the same order of magnitude [16]. Similar thermodynamics, as outlined below, should, therefore, also be applicable to these entities. Note that hydrostatic pressures of the order of magnitude 10 GPa are known to lead to structural transformations in strongly covalent group IV and III-V semiconductors [17].

Since the transition temperature from bulk β-Sn to α-Sn is with 286 K just a few degrees below room temperature, we can (for comparisons of the Gibbs free energies (G) of both phases at room temperature) in a first approximation assume that the differences between internal energies (E) and the products of entropies (S) and temperature ($T \approx 300$ K) are equal for both phases in the bulk. If we assume further that the homogenous contributions to the interface energies between Sn and Si ($I_{Sn/Si}$) are about equal for both phases and that the $B_{\beta\text{-Sn}}\ \Delta V_{\beta\text{-Sn}}$ product is for β-Sn precipitates negligible due to mismatch strain minimizing orientation relationships, e.g. Fig. 4b, we are left with only two significant energy terms to determine if a phase transition from an α-Sn quantum dot to a precipitate with β-Sn structure is thermodynamically favorable.

These significant energy terms are the total excess Gibbs free energy that arises from the large elastic mismatch energy ($B_{\alpha\text{-Sn}}\ \Delta V_{\alpha\text{-Sn}}$) of the α-Sn QD and the incoherent

contribution to the interface energy between the β-Sn precipitate and the Si matrix (I_{inc}). As the excess Gibbs free energy totals about 9.6 keV for the model α-Sn QD, and the incoherent contribution to the interface energy between the β-Sn precipitate and the Si matrix may be estimated from dislocation models of interfaces to be at most of the order of magnitude 0.1 keV, we can safely conclude (under the above given assumptions) that the balance between the Gibbs free energies of both phases

$$E_{\beta\text{-Sn}} - T\,S_{\beta\text{-Sn}} + B_{\beta\text{-Sn}}\,\Delta V_{\beta\text{-Sn}} + I_{\beta\text{-Sn/Si}} + I_{inc} < E_{\alpha\text{-Sn}} - T\,S_{\alpha\text{-Sn}} + B_{\alpha\text{-Sn}}\,\Delta V_{\alpha\text{-Sn}} + I_{\alpha\text{-Sn/Si}}$$

supports the assumed structural transformation. Note also that β-Sn has a 26 % higher density than α-Sn, making it intuitively apparent that a structural transition to the β-Sn prototype must result in a significant reduction of the elastic mismatch energy [13].

So far we only observed β-Sn structure precipitates at or close to the level of the former Sn_xSi_{1-x} layer from which the solid substitutional Sn_ySi_{1-y} precipitates grew. This observation seems to suggest that it is only these entities that transform into β-Sn precipitates within a few years. Although the precipitates that grow by the void mediated formation mechanism consist (possibly) of pure α-Sn, i.e. have potentially a high elastic mismatch energy, there might be a balance between this energy that builds up gradually as the voids get filled and the energy gained by precipitation from the adjacent substitutional Sn_zSi_{1-z} ($z << x$) solution from which the Sn depletes. This balance may prevent the build up of too large an elastic mismatch energy and result in such precipitates being structurally stable or at least metastable for many years.

4. CONCLUSIONS

The thermodynamics of misfitting precipitates provide reasonable explanations for structural and morphological transformations of Sn (rich) quantum dots in Si matrix that were observed by means of analytical transmission electron microcopy. Electron microscopical experiments at elevated temperatures are needed to clarify if our observations on β-Sn structure precipitates are statistically significant and if QDs that formed by the void mediated mechanism are structurally stable.

ACKNOWLEDGMENTS

The TEM analyses were supported by both a grant to PM by the Campus Research Board of the University of Illinois at Chicago and a grant to NDB by NSF (DMR-9733895). The growth of Sn_xSi_{1-x}/Si multi-quantum well structures was supported by a NSF grant (ECS-0103543) to HAA.

REFERENCES

[1] R.A. Soref and C.H. Perry, *J. Appl. Phys.* **69**, 539 (1991).

[2] M.F. Flyn, J. Chevallier, J. Lundsgaard Hansen, and A. Nylandsted Larsen, *J. Vac. Sci. Technol. B* **16**, 1777 (1998).

[3] M.F. Flyn, J. Chevallier, A. Nylandsted Larsen, R. Feidenhans'l, and M. Seibt, *Phys. Rev. B* **60**, 5770 (1999).

[4] C. Ridder, M. Fanciulli, A. Nylandsted Larsen, and G. Weyer, *Mater. Sci. Semicond. Processing* **3**, 251 (2000).

[5] K.S. Min and H.A. Atwater, *Appl. Phys. Lett.* **72**, 1884 (1998).

[6] R. Ragan, K.S. Min, and H.A. Atwater, *Mater. Sci. Engin. B* **87**, 204 (2001).

[7] P. Möck, Y. Lei, T. Topuria, N.D. Browning, R. Ragan, K.S. Min, and H.A. Atwater, *Proc. 47th Annual Meeting of The International Society for Optical Engineering (SPIE),* July 7-11, 2002, Seattle, WA.

[8] P. Möck, Y. Lei, T. Topuria, N.D. Browning, R. Ragan, K.S. Min, and H.A. Atwater, *Proc. 2nd Intern. Workshop on Quantum Nanostructures & Nanoelectronics*, pp. 241 – 246, AIST-Tsukuba Research Center, September 9-11, 2002, Tsukuba, Japan

[9] Y. Lei, P. Möck, T. Topuria, N.D. Browning, R. Ragan, K.S. Min, and H.A. Atwater, *submitted to Phys. Rev. B.*

[10] D.J. Eaglesham, A.E. White, L.C. Feldman, N. Moriya, and D.C. Jacobson, *Phys. Rev. Lett.* **70**, 1643 (1993).

[11] W.C. Johnson, "Influence of Elastic Stress on Phase Transformations", in: *Lectures on the Theory of Phase Transformations*, 2nd Edition, (Ed. H.I. Aaronson, The Minerals, Metals & Materials Society, Warrendale, 2001).

[12] R.E. Miller and V.B. Shenoy, *Nanotechnology* **11**, 139 (2000).

[13] Assuming standard lattice constants for Si and β-Sn (i.e. assuming that this precipitate is not a substitutional solution of Sn and Si with β-Sn structure), these parallel vector pairs are calculated to agree in length within 2.8 % for the first pair, 1.2 % for the second pair, and 0.9 % for the final pair. If this precipitate were to consist of pure Sn, it would be under compressive strain of the order of magnitude 1 %. It is, however, impossibly to decide from analytical TEM for specimens of the present kind if the precipitate consists of pure Sn or if there may be a Si substitutional solution content that would result in other strain values (of possibly the opposite sign).

[14] $\frac{4}{m}\bar{3}\frac{2}{m} \cap \bar{1}\bar{1}\frac{2}{m} = \bar{1}\bar{1}\frac{2}{m}$, which is the point symmetry of a rhombic dipyramidal polyhedron.

[15] It is assumed that both the precipitate and the matrix (in the immediate vicinity of the precipitate) are deformed according to the ratio of their bulk moduli, resulting in a perfect lattice parameter match at the interface.

[16] With the same starting parameters as above, one obtains for, e.g., a $Sn_{0.5}Si_{0.5}$ QD (bulk modulus 70.2 GPa, from Vegard's law), with a strained lattice constant of 0.56519 nm [15], an elastic mismatch energy of 0.27 eV per atom, corresponding to a hydrostatic pressure of 12.1 GPa.

[17] G.J. Ackland, *Rep. Prog. Phys.* **64**, 483 (2001).